Observability and Detectability Analyses for Dynamic State Estimation of the Marginally Observable Model of a Synchronous Machine

Ning Zhou^{1*}, Shaobu Wang², Junbo Zhao³, Zhenyu Huang², Renke Huang²

Abstract: Observability and detectability analyses are often used to guide the measurement setup and select the estimation models used in dynamic state estimation (DSE). Yet, marginally observable states of a synchronous machine prevent the direct application of conventional observability and detectability analyses in determining the existence of a DSE observer. To address this issue, the authors propose to identify the marginally observable states and their associate eigenvalues by finding the smallest perturbation matrices that make the system unobservable. The proposed method extends the observability and detectability analyses to marginally observable estimation models, often encountered in the DSE of a synchronous machine. The effectiveness and application of the proposed method are illustrated on the IEEE 10-machine 39-bus system, verified using the unscented Kalman filter and the extended Kalman filter, and compared with conventional methods. The proposed analysis method can be applied to guide the selection of estimation models and measurements to determine the existence of a DSE observer in power-system planning.

Nomenclature		n	Number of dynamic system states.		
		N/A	Not applicable.		
(·)*	Optimal solution of (·).	p	Number of dynamic system inputs.		
€	Element of.	P_e	Real power.		
≜	Equal by definition.	PFs	Participation factors.		
0_A , 0_C	Zero-value submatrices of A and C.	q	Normalized right eigenvector.		
A, B, C, D	Jacobian matrices of the dynamic system in the	Q_e	Reactive power.		
$\bar{A}, \bar{B}, \bar{C}, \bar{D}$	observability staircase form. Jacobian matrices of the dynamic system after	r	Number of observable states.		
A	linearization. Two-norm of matrix <i>A</i> .	$\mathbb{R}^{n \times m}$	Real-number matrix set of size $n \times m$.		
A^H	Conjugate transpose of matrix A.	$rank(\cdot)$	Operation of finding the rank of a matrix.		
A^T	Transpose of matrix A .	$S_R(\cdot)$	Set of perturbation matrices that make the model unobservable.		
$A_k(i:j,k:l)$	Submatrix of A_k formed by its elements on rows i through j and columns k through l .	t	Current time.		
$A_k(i:j,:)$	Submatrix of A_k formed by its rows i through j .	T_M, P_{SV}	Mechanical torque and steam valve position the turbine-governor model, respectively.		
A_{mo} , A_o	Submatrices of A for marginally observable	T_{q0}'	Time constant of E'_d .		
$\mathbb{C}^{n \times m}$	states and observable states, respectively. Complex-number matrix set of size $n \times m$.	U	Unitary matrix for transforming the system into the observability staircase form.		
E_{fd}, V_F, V_R	Field voltage, stabilizing transformer output,	ν	Voltage phasor.		
	and amplifier output of the exciter, respectively.	x(t)	State vector after transformation into the observability staircase form.		
$eig(\cdot)$	Operation of finding eigenvalues.	$\bar{x}(t)$	State vector after linearization.		
${\mathcal I}$	Current phasor.	$\hat{\chi}(t)$	Estimated state of $x(t)$.		
I_n	Identity matrix of size $n \times n$.	x_{mo}, \hat{x}_{mo}	Marginally observable states and their		
K	Kalman gain.	x_o, \hat{x}_o	estimates. Observable states and their estimates.		
m	Number of system outputs.				
		y(t)	Output vector of the dynamic system.		

¹ Electrical and Computer Engineering Department, Binghamton University, Binghamton, NY 13902, USA

² Pacific Northwest National Laboratory, Richland, WA 99354, USA

³ Electrical and Computer Engineering Department, Mississippi State University, Starkville, MS 39759, USA *ningzhou@binghamton.edu

 $\delta, \omega, E'_d, E'_q$ Rotor angle, rotor speed, and d-axis and q-axis transient voltages of a generator, respectively. $\Delta \bar{A}, \Delta \bar{C}$ Perturbation matrices of \bar{A} and \bar{C} . $\Delta x(t)$ Difference between $\hat{x}(t)$ and x(t). $\varepsilon, \varepsilon'$ Thresholds of distance and relative distance for determining observability. λ Eigenvalue. μ_R, μ'_R Shortest distance and relative shortest distance to an unobservable system, respectively.

1. Introduction

Dynamic state estimation (DSE) has been used to estimate the dynamic states of power systems [1] [2]. To ensure the existence of a DSE observer, it is important to properly select inputs/outputs of estimation models [3]. Observability and detectability analyses have been used to determine whether a DSE observer exists [4]- [5] for a selected estimation model and guide measurement selection [6].

Observability analysis determines whether the initial states can be uniquely determined [4]. To apply one of the well-established observability analysis methods used for linear systems, a nonlinear system is linearized around an operating point to calculate the observability matrix [7]. Previous work pointed out that observability based on linearization is only a local property of a nonlinear system around an equilibrium point instead of a global property [8]. In some highly nonlinear scenarios, applying the Lie derivative to construct the observability matrix provides a more accurate estimate at the cost of increased computational complexity [7]. For a high-order model in power systems, the computational complexity of the Lie derivative can be mitigated by using an automatic differentiation technique [9] [10]. The above methods require an analytical model to derive the observability matrix. To relax that requirement, Qi [11] and Sun [5] et al. use the empirical observability Gramian matrix to quantify observability. Observability is a sufficient condition to guarantee the existence of a DSE observer.

In the DSE of a power system, it was noted in [12] that some DSE observers converged even if their estimation models were not observable. The result suggests that the requirement from observability analysis is conservative and may call for additional unnecessary measurements. Leveraging detectability analysis, Zhou et al. [12] have relaxed the observability requirement by showing that a DSE observer converges not only for an observable system but also for an unobservable system as long as the eigenvalues corresponding to the unobservable states are stable. Detectability analysis determines whether estimated states can asymptotically converge to their true values as time passes by [13]. As such, detectability is a more relaxed condition than observability for determining the existence of a DSE observer. Applying detectability analysis has the potential to reduce the number of measurements required by an observability analysis for determining the existence of a DSE observer.

These conventional observability and detectability analysis methods have laid solid groundwork for selecting inputs/outputs and placing measurements for DSE in power systems. Yet, they cannot determine the existence of a DSE observer for a synchronous machine with marginally observable states. While conventional methods can detect a marginally observable system by checking the smallest singular value (SSV) and the condition number of the observability matrix, they cannot identify the marginally observable states and their associate eigenvalues. As a result, these conventional methods cannot determine whether marginally observable states have stable eigenvalues and, in turn, whether the marginally observable states will lead to the divergence of a DSE observer.

To overcome the limitation of conventional methods applied to a marginally observable model, the authors of this paper propose an extended observability and detectability method by identifying the marginally observable states and their associate eigenvalues. To do so, the smallest perturbation that can make the original system unobservable is calculated using the algorithms in [14]. Then, the model is transformed into staircase form through the Kalman decomposition. The staircase form allows the marginally observable states to be separated from the observable states in observability analysis [13] and for their corresponding eigenvalues to be identified for detectability analysis. Through this procedure, the proposed method extends the application of observability and detectability analyses to marginally observable systems, which are quite common in DSE with a high-order synchronous machine model.

The rest of this paper is organized as follows. The method to identify marginally observable states and their associated eigenvalues is introduced in Section 2. The application of the proposed method in power systems is discussed in Section 3. Case studies are carried out in Section 4. Finally, conclusions are drawn in Section 5.

2. Quantification of Observability and Identification of Marginally Observable States

To apply the proposed method, a nonlinear model in power systems needs to be linearized into (1) around its operation points for observability and detectability analyses.

$$\frac{d\bar{x}(t)}{dt} = \bar{A}\bar{x}(t) + \bar{B}u(t)$$
 (1.a)

$$y(t) = \bar{C}\bar{x}(t) + \bar{D}u(t) \tag{1.b}$$

Here, $\bar{x}(t) \in \mathbb{R}^{n \times 1}$ is the state vector at time t, $u(t) \in \mathbb{R}^{p \times 1}$ is the input vector, and $y(t) \in \mathbb{R}^{m \times 1}$ is the output vector; and $\bar{A} \in \mathbb{R}^{n \times n}$, $\bar{B} \in \mathbb{R}^{n \times p}$, $\bar{C} \in \mathbb{R}^{m \times n}$, and $\bar{D} \in \mathbb{R}^{m \times p}$ are the corresponding Jacobian matrices.

2.1. Distance to Unobservability

The observability of model (1) can be quantified by $\mu_R(\bar{A}, \bar{C})$ defined in (2), which is the shortest distance of (1) to an unobservable model.

$$\mu_{R}(\bar{A},\bar{C}) \triangleq \min \left\{ \left\| \frac{\Delta \bar{A}}{\Delta \bar{C}} \right\| : \begin{array}{c} (\bar{A} + \Delta \bar{A},\bar{C} + \Delta \bar{C}) \\ is \ unobservable \end{array} \right\} \tag{2}$$

Here, $\|\cdot\|$ denotes the 2-norm of the matrix [15]; $\Delta \bar{A} \in \mathbb{R}^{n \times n}$ and $\Delta \bar{C} \in \mathbb{R}^{m \times n}$ are the perturbation matrices. Obviously, if $\mu_R(\bar{A}, \bar{C}) = 0$, (1) is unobservable.

To find $\mu_R(\bar{A}, \bar{C})$, the controllability studies carried out by [14] are adopted for observability studies using their duality. In particular, it has been shown that the distance defined in (2) is equivalent to (3), where $\lambda \in \mathbb{C}^{1\times 1}$. Note that

the unobservability condition in (2) is converted into the condition of rank deficiency of the constructed matrix at every eigenvalue, λ , of the perturbed matrix $\bar{A} + \Delta \bar{A}$ in (3.b)

$$\mu_{R}(\bar{A}, \bar{C}) = \min_{\lambda \in \mathbb{C}^{1 \times 1}} \left\{ \min_{\substack{\left[\Delta \bar{A} \\ \Delta \bar{C}\right] \in S_{R}(\lambda)}} \left(\left\| \frac{\Delta \bar{A}}{\Delta \bar{C}} \right\| \right) \right\}$$
(3.a)

$$\mu_{R}(\bar{A}, \bar{C}) = \min_{\lambda \in \mathbb{C}^{1 \times 1}} \left\{ \min_{\substack{\left[\Delta \bar{A} \\ \Delta \bar{C} \right] \in S_{R}(\lambda)}} \left(\left\| \Delta \bar{A} \right\| \right) \right\}$$

$$S_{R}(\lambda) = \left\{ \begin{array}{c} \left[\Delta \bar{A} \\ \Delta \bar{C} \right] \in \mathbb{R}^{(n+m) \times n} \\ : rank \left[\bar{A} + \Delta \bar{A} - \lambda I_{n} \\ \bar{C} + \Delta \bar{C} \right] < n \right\}$$
(3.a)

Furthermore, the distance can be reformulated as $\mu_R(\bar{A},\bar{C}) =$

$$\min_{q \in \{\mathbb{R}^{n \times 1} \cup \mathbb{R}^{n \times 2}\}} \left\{ \left\| \begin{pmatrix} (I_{\overline{2}} - qq^{T}) \bar{A}q \\ \bar{C}q \end{pmatrix} \right\| \right\}$$
 where $q^{T}q = I_{\widetilde{2}} \in \mathbb{R}^{1 \times 1}$ or $\mathbb{R}^{2 \times 2}$ and $I_{\widetilde{2}}$ is an identity

matrix.

Exploiting the duality of controllability and observability, $\mu_R(\bar{A}, \bar{C})$ and its associated q can be obtained. Once the optimal solution $q = q^*$ is found, the corresponding eigenvalues $\lambda = \lambda^*$ can be calculated via (5).

$$\lambda^* = eig(q^{*T}\bar{A}q^*) \tag{5}$$

When $q^* \in \mathbb{R}^{n \times 1}$, λ^* is a real scalar that is associated with the solution of (3); when $q^* \in \mathbb{R}^{n \times 2}$, λ^* represents a pair of complex conjugate eigenvalues that are associated with the solution of (3). After λ^* and q^* are found, the perturbation matrices $\Delta \bar{A}^*$ and $\Delta \bar{C}^*$ can be obtained from (6).

$$\Delta \bar{A}^* = -\{I_n - q^* q^{*T}\} \bar{A} q^* q^{*T}$$
(6.a)

$$\Delta \bar{C}^* = -\bar{C} q^* q^{*T} \tag{6.b}$$

Here, $I_n \in \mathbb{R}^{n \times n}$ is an identity matrix. The algorithms and the corresponding derivations are summarized in Appendix A.

Note that when $\mu_R(\bar{A}, \bar{C}) = 0$ the system is unobservable. This is equivalent to that from the study on the observability matrix [4] and conventional methods can be directly applied to determine the existence of DSE observers. Yet, when $\mu_R(\bar{A}, \bar{C})$ is very small, some states in the models are marginally observable (i.e., effectively unobservable) and conventional methods cannot directly determine whether a DSE observer exists. This calls for an extended method to separate marginally observable states from fully observable states.

2.2. Marginally Observable States and Their Eigenvalues

A system is marginally observable if it is very close to an unobservable system. The shortest distance from the studied system to an unobservable system is a numerically robust metric to quantify the observability of a dynamical system and identify a marginally observable system [15] [16]. Thresholds ε and ε' can be set up for the distance (7.a) and relative distance (7.b) to determine whether the system described by (1) is marginally observable.

$$0 < \mu_R(\bar{A}, \bar{C}) < \varepsilon \tag{7.a}$$

$$0 < \mu'_{R}(\bar{A}, \bar{C}) \triangleq \frac{\mu_{R}(\bar{A}, \bar{C})}{\left\|\bar{A} - \lambda^{*} I_{n}\right\|} < \varepsilon'$$
(7.b)

Here, (7.a) is more suitable for models quantified with absolute errors, while (7.b) is more suitable for models quantified with relative errors.

When (1) is marginally observable, i.e., (7) holds, the marginally observable states can be separated from the observable states by transforming the perturbed system into the observability staircase form using the Kalman decomposition for observability [13]. More specifically, a unitary matrix $U \in \mathbb{R}^{n \times n}$ can be found to transform $\{\bar{A} + A\}$ $\Delta \bar{A}^*, \bar{B}, \bar{C} + \Delta \bar{C}^*, \bar{D}$ into (8) through the similarity transform defined by (9).

$$\begin{bmatrix} \frac{dx_{mo}(t)}{dt} \\ \frac{dx_{o}(t)}{dt} \end{bmatrix} = \begin{bmatrix} A_{mo} & A_{12} \\ 0_A & A_o \end{bmatrix} \begin{bmatrix} x_{mo}(t) \\ x_o(t) \end{bmatrix} + \begin{bmatrix} B_{mo} \\ B_o \end{bmatrix} u(t)$$
(8.a)

$$y(t) = \begin{bmatrix} 0_C & C_o \end{bmatrix} \begin{bmatrix} x_{mo}(t) \\ x_o(t) \end{bmatrix} + [D]u(t)$$
 (8.b)

$$\bar{x}(t) = U^T x(t) \tag{9.a}$$

$$x(t) \triangleq \begin{bmatrix} x_{mo}(t) \\ x_o(t) \end{bmatrix}$$
 (9.b)

Here, $x_{mo}(t) \in \mathbb{R}^{(n-r)\times 1}$ and $x_o(t) \in \mathbb{R}^{r\times 1}$ respectively represent the marginally observable (mo) state vector and the observable (o) state vector; $A_{mo}(t) \in \mathbb{R}^{(n-r)\times(n-r)}, A_o(t) \in \mathbb{R}^{r\times r}$, $A_{12}(t) \in \mathbb{R}^{(n-r)\times r}$, $0_A \in \mathbb{R}^{r\times(n-r)}$, $B_{mo}(t) \in \mathbb{R}^{(n-r)\times p}$, $B_o(t) \in \mathbb{R}^{r\times p}$, $0_C \in \mathbb{R}^{m\times(n-r)}$, and $C_o \in \mathbb{R}^{m\times r}$ are the corresponding transformed submatrices. Note that 0_A is a zero matrix, which suggests that $x_o(t)$ is not influenced by $x_{mo}(t)$. Also, 0_C is a zero matrix, which suggests that y(t) is not influenced by $x_{mo}(t)$. As such, the eigenvalues corresponding to the marginally observable state are the eigenvalues of A_{mo} in (8.a).

2.3. Observers and Detectability Analysis on Marginally Observable Systems

For a system described by (8), an observer can be formed from measured inputs and outputs using (10) [17] for the DSE. Here, $\hat{x}(t) \triangleq [\hat{x}_{mo}(t)^T \ \hat{x}_o(t)^T]^T \in \mathbb{R}^{n \times 1}$ is the estimate of x(t); $K \in \mathbb{R}^{n \times m}$ is a design parameter, $K_{mo} \triangleq K(1:n-r,:) \in \mathbb{R}^{(n-r) \times m}$, $K_o \triangleq K(n-r+1:n,:) \in$ $\mathbb{R}^{r \times m}$. In the DSE within the Kalman filter framework, K is the Kalman gain that minimizes the estimation variance for the unbiased estimate [17]. The estimation errors are defined $\Delta x(t) = \hat{x}(t) - x(t)$. The dynamical model of the estimation errors can be written as (11) by first taking the difference between (8.a) and (10.b), then substituting y(t) (8.b)into the resulting equation.

$$\frac{d\hat{x}(t)}{dt} = A\hat{x}(t) + Bu(t) + K\{y(t) - C\hat{x}(t) - Du(t)\}$$
(10.a)

$$\begin{bmatrix} \frac{d\hat{x}_{mo}(t)}{dt} \\ \frac{d\hat{x}_{o}(t)}{dt} \end{bmatrix} = \begin{bmatrix} A_{mo} & A_{12} - K_{mo}C_{o} \\ 0_{A} & A_{o} - K_{o}C_{o} \end{bmatrix} \begin{bmatrix} \hat{x}_{mo}(t) \\ \hat{x}_{o}(t) \end{bmatrix} + \begin{bmatrix} K_{mo} \\ K_{o} \end{bmatrix} y(t) + \begin{pmatrix} B_{mo} \\ B_{o} \end{pmatrix} - \begin{bmatrix} K_{mo} \\ K_{o} \end{bmatrix} D u(t)$$

$$(10.b)$$

$$\begin{bmatrix}
\frac{d\Delta x_{mo}(t)}{dt} \\
\frac{d\Delta x_o}{dt}
\end{bmatrix} = \begin{bmatrix}
A_{mo} & A_{12} - K_{mo}C_o \\
0 & A_o - K_oC_o
\end{bmatrix} \begin{bmatrix}
\Delta x_{mo}(t) \\
\Delta x_o(t)
\end{bmatrix}$$
(11)

According to the detectability analysis [12], the convergence properties of the DSE depend on the stability and observability of the states. For the observable states $\hat{x}_o(t)$, K in (11) can be selected to place the eigenvalues of A_o – $K_o C_o$ at the left half of the s-plane to make them stable [18] such that the estimation errors of $\Delta x_o(t)$ will converge to zero. By contrast, the eigenvalues of the marginally observable states $\hat{x}_{mo}(t)$ are determined by A_{mo} and cannot be effectively controlled by K. The estimation errors of $\Delta \hat{x}_{mo}(t)$ will increase if any eigenvalue of A_{mo} is unstable and otherwise be damped out if all the eigenvalues of A_{mo} are stable. Thus, the convergence of the marginally observable states in the DSE is mainly determined by the damping of the right-most eigenvalues of A_{mo} . If all the eigenvalues of A_{mo} are stable, there shall exist a DSE observer for the marginally observable model. If any eigenvalues of A_{mo} are unstable, the DSE shall diverge.

3. Applications of the Proposed Method in the **Power System DSE**

The proposed method can be used to determine whether a DSE observer exists for different estimation models of a synchronous machine. First, estimation models for the DSE of a synchronous machine are discussed to show the different options available to users. Then, the application procedure of the proposed method is summarized.

3.1. Estimation Models

The dynamic model of a synchronous generator and its associated controllers used in this paper are described by the ninth-order ordinary differential equations (ODEs) in (12)-(20) [19] [20]. Here, δ , ω , E'_d , and E'_q are the rotor angle, rotor speed, and d-axis and q-axis transient voltages of the generator, respectively; E_{fd} , V_F , and V_R are the field voltage, the stabilizing transformer output, and the amplifier output of the exciter, respectively; T_M and P_{SV} are the mechanical torque and steam valve position of the turbine-governor model, respectively; P'_{e} is the real power generated by the generator; V_{ref} and P_C are the control reference signals of the exciter and governor, respectively.

Generator's ODEs:

$$\frac{d\delta}{dt} = \omega - \omega_s,\tag{12}$$

$$\frac{d\omega}{dt} = \frac{\omega_s}{2H} \left(T_M - P'_e - D(\omega - \omega_s) \right), \tag{13}$$

$$\frac{dE'_q}{dt} = \frac{1}{T'_{d0}} \left(-E'_q - (X_d - X'_d)I_d + E_{fd} \right), \tag{14}$$

$$\frac{dE'_d}{dt} = \frac{1}{T'_{q0}} \left(-E'_d - (X_q - X'_q)I_q \right). \tag{15}$$

Exciter's ODEs.

$$\frac{dE_{fd}}{dt} = \frac{1}{T_E} \left(-\left(K_E + S_E (E_{fd}) \right) E_{fd} + V_R \right), \tag{16}$$

$$\frac{dV_{F}}{dt} = \frac{1}{T_{F}} \begin{pmatrix} -V_{F} + \frac{K_{F}}{T_{E}} V_{R} \\ -\frac{K_{F}}{T_{F}} \left(K_{E} + S_{E} \left(E_{fd} \right) \right) E_{fd} \end{pmatrix}, \tag{17}$$

$$\frac{dV_R}{dt} = \frac{1}{T_A} \left(-V_R + K_A \left(V_{ref} - V_F - V \right) \right). \tag{18}$$

Turbine-governor's ODEs:

$$\frac{dT_{M}}{dt} = \frac{1}{T_{CH}} (-T_{M} + P_{SV}), \tag{19}$$

$$\frac{dP_{SV}}{dt} = \frac{1}{T_{SV}} \left(-P_{SV} + P_C - \frac{1}{R_D} \left(\frac{\omega}{\omega_S} - 1 \right) \right). \tag{20}$$

Assume that the voltage phasor $(\mathcal{V} = V_R + jV_I)$ and current phasor $(\mathcal{I} = I_R + jI_I)$ are measured using a PMU at the terminal bus of the synchronous machine. Also, the real power (P_e) and reactive power (Q_e) injected to the generator can be calculated from the voltage and current phasors through $P_e + jQ_e = \mathcal{VI}^*$ and used as measurements. In addition, V_{ref} and P_C are available to DSE. There are several ways of setting up input, u(t), and output, y(t), of the estimation model (1).

3.1.1 Models using Voltage Phasors as Inputs

One way of setting up the estimation model is to use the voltage phasor as its input, i.e., u(t) = $[V_R \ V_I \ V_{ref} \ P_C]^T$. When the current phasor is also available, real power (P_e) and reactive power (Q_e) are used as model output, i.e., $y(t) = [P_e \ Q_e]^T$ (denoted as model a henceforward). When the current phasor is not available because of sensor failure or maintenance, model output can be set as null, i.e., y(t) = [] (denoted as model b henceforward).

In this setup, the generated real power P'_{e} in (13) can be constructed from the voltage phasor and dynamic states using (21) and (22). In (21), I_d , I_q , V_d , and V_q are the intermediate variables, which can be calculated from the voltage phasor and states using (22). I_d and I_q are the *d*-axis and q-axis armature currents, respectively; V_d , V_q are the daxis and q-axis terminal voltages, respectively.

$$P'_{e} = (E'_{d} + I_{q}X'_{q})I_{d} + (E'_{q} - I_{d}X'_{d})I_{q}$$
(21)

$$V_d = V_R \sin \delta - V_I \cos \delta \tag{22.a}$$

$$V_q = V_R \cos \delta - V_I \sin \delta \tag{22.b}$$

$$I_d = \frac{E_q' - V_q}{V'} \tag{22.c}$$

$$I_d = \frac{E'_q - V_q}{X'_d}$$
 (22.c)
 $I_q = -\frac{E'_d - V_d}{X'_q}$ (22.d)

The output of real power (P_e) and reactive power (Q_e) in model a can be calculated from the voltage phasor and states using (22) and (23).

$$P_e = V_d I_d + V_q I_q \tag{23.a}$$

$$Q_e = -V_d I_q + V_q I_d \tag{23.b}$$

3.1.2 Models using Current Phasors as Inputs

Another way of setting up the estimation model is to the current phasor as its input, i.e., u(t) = $[I_R \ I_I \ V_{ref} \ P_C]^T$. When the voltage phasor is also available, real power (P_{ρ}) and reactive power (Q_{ρ}) are used as model output, i.e., $y(t) = [P_e \quad Q_e]^T$ (denoted as model c henceforward); When the voltage phasor is not available because of sensor failure or maintenance, model output can be set as null, i.e., y(t) = [] (denoted as model d henceforward).

In this setup, the generated real power P'_{e} in (13) can be constructed from the current phasor and dynamic states using (21) and (24). The output of real power (P_e) and

reactive power (Q_e) in *model c* can be calculated from the current phasor and states using (23) and (24).

$$I_d = I_R \sin \delta - I_I \cos \delta \tag{24.a}$$

$$I_q = I_R cos\delta - I_I sin\delta \tag{24.b}$$

$$V_d = E_d' + I_q X_q' \tag{24.c}$$

$$V_q = E_q' - I_d X_d' \tag{24.d}$$

Note that in addition to the four models discussed above, there are many other ways of setting up estimation models for DSE with the same measurements. For example, Fan et al. [21] proposed an estimation model that uses real power and reactive power as its input and the voltage phasor as its output. With many estimation models available, users need a method to determine whether an estimation model can ensure the existence of a DSE observer.

3.2. Application of the Proposed Method

In order to apply the proposed method to determine whether a DSE observer exists for different estimation models of a synchronous machine, the procedure illustrated by the flow chart in Fig. 1 should be followed. The chart suggests that if a model has a marginally observable or unobservable state whose eigenvalues are not stable, the corresponding DSE will diverge. In addition, a stable model is preferred for DSE because a stable model will guarantee the convergence of the DSE whether the system is observable, marginally observable, or unobservable. Note that Steps 5 and 6 in the flow chart are the distinguishing features of the proposed method in that it can be applied to a marginally observable model while conventional methods cannot.

4. Case Studies

Application examples are presented in this section to illustrate the properties and value of the proposed method in guiding the selection of estimation models for DSE. Specifically, the proposed method is applied to determine the existence of a DSE observer for several different estimation models of a synchronous machine in the IEEE 10-machine 39-bus system [22] [23] shown in Fig. 2. To verify the analysis results of the proposed method, DSE is carried out using the unscented Kalman filter (UKF) [20] and the extended Kalman filter (EKF) [21] to reveal their convergence properties. In addition, the detectability analysis [12] and the observability analysis using the empirical Gramian [11] [5], linearization [7], and the Lie derivative [7] [9] [10] are carried out to reveal the distinguishing features of the proposed method.

4.1. Simulation Setup

The IEEE 10-machine 39-bus system is used to generate simulation data. To simulate dynamic responses, the transmission line between bus 16 and bus 21 is tripped off at 20 s. The system responses are recorded for 80 s. A phasor measurement unit (PMU) is assumed to be installed at the terminal bus of synchronous machine G5 and measures the voltage phasor (\mathcal{V}) and current phasor (\mathcal{I}) at 60 samples/s. One percent measurement noise in total vector error is added to the measured phasors. The corresponding real power (P_e) and reactive power (Q_e) are calculated from \mathcal{V} and \mathcal{I} . The

measurements allow the application of the four estimation models discussed in the previous section for DSE.

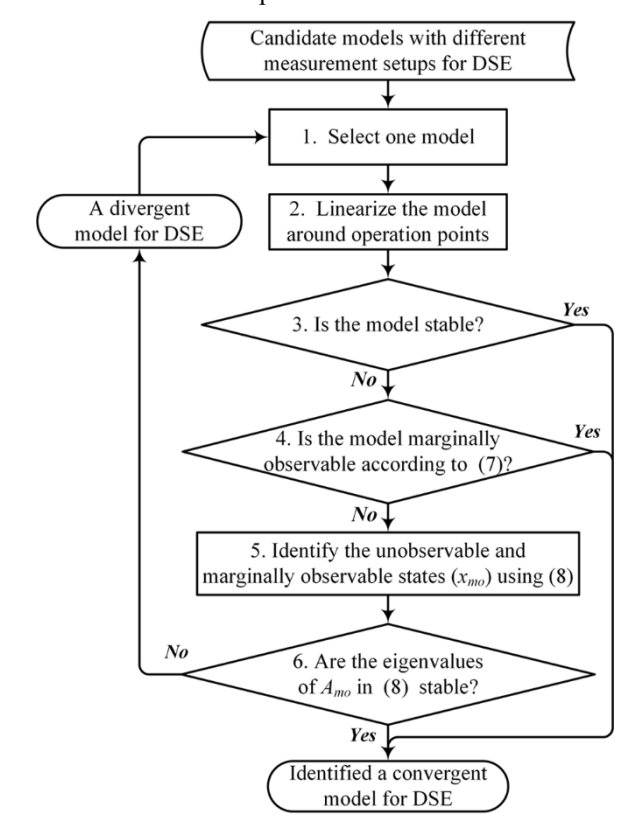


Fig. 1. Flow chart of using the proposed method to select a convergent estimation model for the DSE

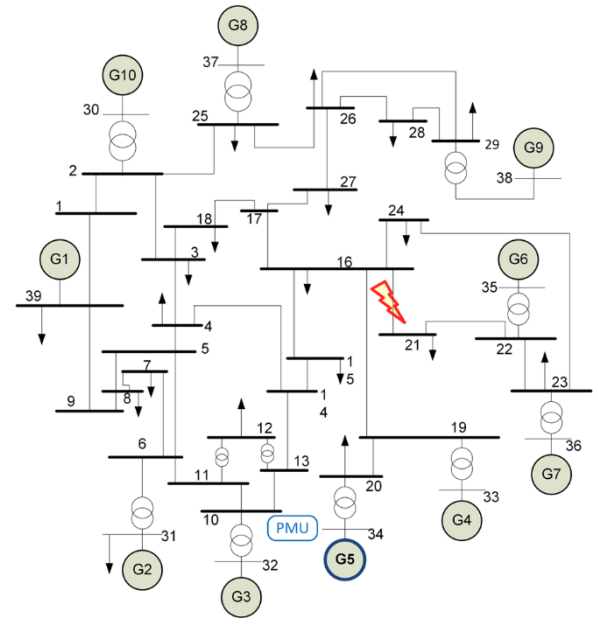


Fig. 2. One-line diagram of the IEEE 10-machine 39-bus system [22]

4.2. Observability and Detectability Analyses using the Proposed Method

Following the procedure described in Fig. 1, the proposed method is applied to determine the existence of a DSE observer for the four estimation models described in subsection III.A. Table 1 summarizes the analysis results. Considering that the relative noise level of the dynamic model

of a synchronous machine is often greater than 0.1%, the relative threshold is set up as $\varepsilon' = 0.1\%$ in (7).

As a result, the observability analysis using the proposed method suggests that cases (b) and (d) are unobservable, while cases (a) and (c) are marginally observable according to (7). To implement step 3, the rightmost eigenvalues of the estimation models are calculated to check the stability of the estimation models. The eigenvalues suggest that estimation models (a) and (b) are stable while estimation models (c) and (d) are unstable. According to step 3, DSE observers shall exist for models (a) and (b). By contrast, the existence of a DSE observer for models (c) and (d) shall be determined using steps 4, 5, and 6 by checking the eigenvalues of the marginally observable and unobservable states as follows:

- For estimation model (c), the rightmost eigenvalue of its marginally observable state is determined to be 0.4820 using (8). Because the rightmost eigenvalue associated with its marginally observable state is stable, there shall exist a DSE observer for model (c) that can converge according to step 6.
- For estimation model (d), the rightmost eigenvalue of its unobservable state is determined to be 1.7641 using (8). Because the rightmost eigenvalue associated with its unobservable state is unstable, there shall not exist a DSE observer for model (d) according to step 6.

Table 1 Observability and detectability analyses of four different estimation models to determine the existence of a DSE

observer using the proposed method (median \pm median absolute deviation)

Estimation Models	(a)	(b)	(c)	(d)
$\mu_{ m R}$	0.0138 ± 0.0001	0 ± 0	0.0135 ± 0.00001	0 ± 0
μ'_{R}	$(1.37 \pm 0.01) \times 10^{-4}$	(N/A)	$(9.37 \pm 0.01) \times 10^{-5}$	(N/A)
System observability ($\varepsilon' = 0.1\%$)	Marginally Observable	Unobservable	Marginally Observable	Unobservable
Rightmost eigenvalue of the model	-0.0606 ± 0.0002	-0.0606 ± 0.0002	1.7641 ± 0.0013	1.7641 ± 0.0013
Stability of the estimation model	Stable	Stable	Not Stable	Not Stable
Rightmost eigenvalue of the unobservable and marginally observable states	-0.4878	-0.0606	-0.4820	1.7641
Stability of the unobservable and marginally observable states	Stable	Stable	Stable	Not Stable
Existence of a DSE observer	Yes	Yes	Yes	No
Convergence of the UKF	Yes	Yes	Yes	No
Convergence of the EKF	Yes	Yes	Yes	No

Table 2 Observability and detectability analyses using conventional methods [5] [7] [9] [10] [11] [12] (median ± median absolute deviation)

Estimation Models		(a)	(b)	(c)	(d)
Observability using Empirical Gramian [5]	SSV	$(7.03 \pm 3.90) \times 10^{-9}$	0 ± 0	$(9.56 \pm 12.90) \times 10^{-9}$	0 ± 0
	Relative SSV	$(1.39 \pm 0.77) \times 10^{-11}$	(N/A)	$(1.45 \pm 1.95) \times 10^{-12}$	(N/A)
	Observability	Marginally Observable	Unobservable	Marginally Observable	Unobservable
	Existence of a DSE observer	No	No	No	No
Observability	SSV	0.0959 ± 0.0007	0 ± 0	0.0357 ± 0.00003	0 ± 0
using	Relative SSV	$(8.32 \pm 0.04) \times 10^{-9}$	(N/A)	$(1.70 \pm 0.002) \times 10^{-8}$	(N/A)
Linearization	Observability	Marginally Observable	Unobservable	Marginally Observable	Unobservable
[7]	Existence of a DSE observer	No	No	No	No
Observability	SSV	0.430 ± 0.020	0 ± 0	Matlab out of memory	0 ± 0
using Lie	Relative SSV	$(3.70 \pm 0.17) \times 10^{-8}$	(N/A)	Matlab out of memory	(N/A)
~	Observability	Marginally Observable	Unobservable	(N/A)	Unobservable
derivative [7] [9] [10]	Existence of a DSE observer	No	No	(N/A)	No
Detectability Analysis [12]	SSV	0.0959 ± 0.0007	0 ± 0	0.0357 ± 0.00003	0 ± 0
	Relative SSV	$(8.32 \pm 0.04) \times 10^{-9}$	(N/A)	$(1.70 \pm 0.002) \times 10^{-8}$	(N/A)
	Rightmost eigenvalues	-0.0606 ± 0.0002	-0.0606 ± 0.0002	1.7641 ± 0.0013	1.7641 ± 0.0013
	Detectability	Yes	Yes	No	No
	Existence of a DSE observer	Yes	Yes	No	No
Convergence of the UKF		Yes	Yes	Yes	No
Convergence of the EKF		Yes	Yes	Yes	No

In summary, a DSE observer exists for estimation models (a), (b), (c) and does not exist for estimation model (d). The above results also suggest that users may prefer estimation models (a) and (b), which use voltage phasor as

their inputs because they guarantee the existence of a DSE estimator whether the current phasor is available or not. In other words, the voltage phasor is a must-have while the current phasor is optional for the existence of a DSE estimator.

When the current phasor is the input, as in model (d), a DSE estimator does not exist when the voltage phasor is not available. This suggests that adding a backup voltage phasor when placing PMUs can act as a preventive strategy to reduce the risk of losing the voltage phasor.

4.3. Verification using the UKF and EKF

To verify the above results, DSE is carried out using the UKF and EKF to estimate the dynamic states of synchronous machine 5. The nine targeted states include four states of its generator $(\delta, \omega_r, E'_d, E'_q)$, three states of its exciter (E_{fd}, V_F, V_R) , and two states of its turbine-governor model (T_M, P_{SV}) . The corresponding state estimates are displayed in Fig. 3. The DSEs for estimation models (a), (b), and (c) converge, while the DSE for model (d) diverges. These convergence properties are also summarized in the last two rows of Table 1.

Note that the convergence properties of the UKF and EKF agree. They are also consistent with the analysis results on the existence of a DSE observer from the proposed method as the existence of a DSE observer is a necessary, but not sufficient, condition of the convergence of a DSE filter (including for the UKF and EKF). In other words, the convergence of the UKF and EKF indicates that there must exist a DSE observer, but the reciprocal is not inherently true. Similarly, if a DSE observer does not exist, the UKF and EKF shall diverge. The consistency verifies the study results of the proposed method.

The proposed method has been successfully applied to other generators and their associated controllers, then verified using the UKF and EKF. These results have been omitted for brevity.

4.4. Comparison with the Conventional Methods

To reveal the distinguishing features of the proposed method, the SSV and relative SSV of the observability matrices from empirical Gramian [11] [5], linearization [7], and Lie derivative [7] [9] [10] are calculated and summarized in Table 2. To facilitate the comparison, the convergence of the UKF and EKF is also shown in the last two rows of Table 2. Here, the relative SSV is defined as the ratio of the SSV to the largest singular value, i.e., the inverse of the condition number. Note that these observability analysis results are consistent and suggest that models (a) and (c) are marginally observable; and that models (b) and (d) are unobservable. Note that these observability methods can successfully explain the divergence of the UKF and EKF on model (d); but they fail to explain the convergence of the DSE using the UKF and EKF on models (a), (b), and (c).

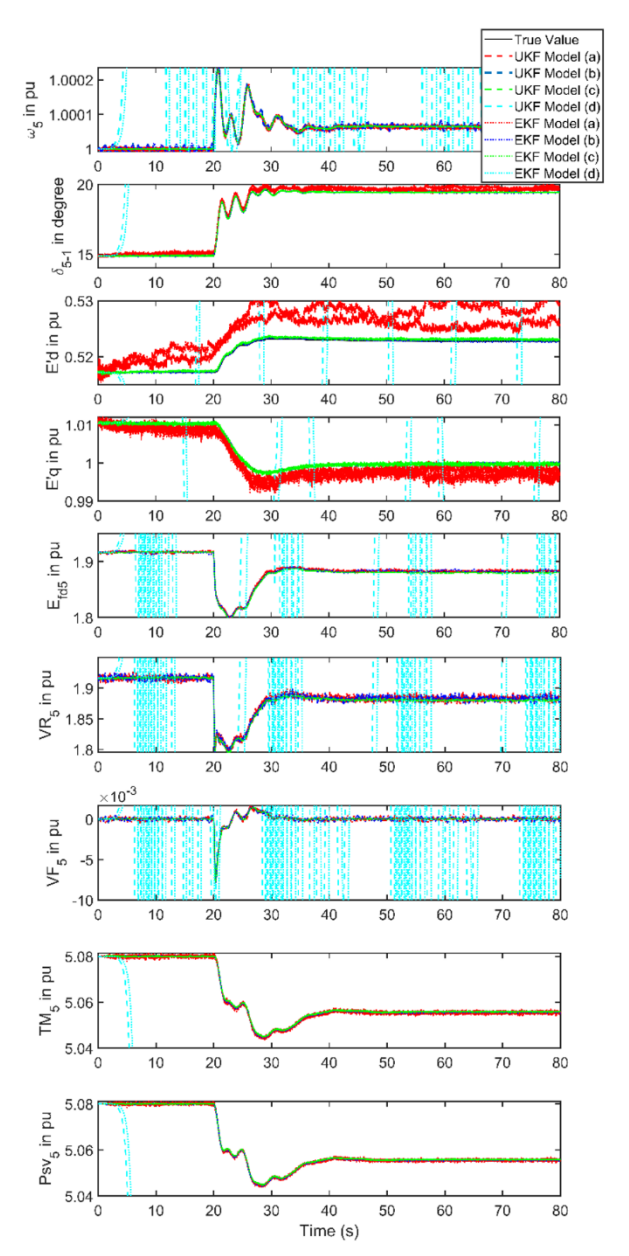


Fig. 3. True and estimated states of machine 5 in the IEEE 10-machine 39-bus system for the four models using the UKF and EKF

Applying the detectability analysis method proposed in [12], models (a) and (b) are detectable because they are stable, while models (c) and (d) are not detectable because they are unstable and effectively unobservable. Note that the detectability method can successfully explain the DSE's divergence on model (d) and convergence on models (a) and (b), but fails to explain the DSE's convergence on estimation model (c). As such, the distinguishing feature of the proposed method is its applicability to a marginally observable model, such as model (c), whose eigenvalues corresponding to its marginally observable states need to be identified.

5. Conclusions

Measurement setup may result in a marginally observable state in estimation models used by the DSE, which often occurs in a high-order synchronous machine model. Conventional observability and detectability analyses cannot be directly applied to a marginally observable system to

determine whether a DSE observer exists for an estimation model. Applying the method proposed here, the smallest perturbation matrices that make the estimation models unobservable are identified and used as a metric to quantify the observability and identify the marginally observable states as well as their associated eigenvalues. It is shown that when all the eigenvalues of the marginally observable states in a synchronous machine are stable, a DSE observer shall exist. When one eigenvalue of the marginally observable states in a synchronous machine is unstable, a DSE observer shall not exist. As such, to ensure the convergence of DSE for a marginally observable system, one shall select measurement setup and estimation models which have stable eigenvalues for marginally observable states unobservable states. The proposed method can identify marginally observable states and their associate eigenvalues, determining their detectability when conventional methods cannot. Because a marginally observable system is often encountered in power system DSE, this advantage allows the proposed method to qualify more estimation models and demand fewer measurements in determining the existence of an observer than the conventional methods.

To leverage the powerful analytical tools available to linear systems, the proposed method uses a linearized model to approximate a nonlinear system around its operating points. As such, the proposed method can be applied to the systems that can be approximated reasonably well by linear models around their operating points. On the other hand, the linearization procedure may introduce linearization errors when the nonlinearity of the system is strong. In future work, the proposed method will be extended to handle the systems with strong nonlinearity.

Appendix A. Find the Minimum Perturbation **Matrices**

The method proposed in [14] is used in this paper to identify the minimum perturbation matrices $\Delta \bar{A}^*$ and $\Delta \bar{C}^*$ that make the original system unobservable. Specifically, the solution to (A1.a) corresponds to a real λ^* while the solution to (A1.b) corresponds to a pair of complex λ^* s. The solution to (4) is obtained as the smaller value of $\mu_{R,1}(\bar{A},\bar{C})$ and $\mu_{R,2}(\bar{A},\bar{C}).$

$$\mu_{R,1}(\bar{A},\bar{C}) = \min_{q \in \mathbb{R}^{n \times 1}} \left\{ \left\| \begin{pmatrix} I_n - qq^T \end{pmatrix} \bar{A}q \\ \bar{C}q \end{pmatrix} \right\}$$
(A1.a)

$$\mu_{R,2}(\bar{A},\bar{C}) = \min_{q \in \mathbb{R}^{n \times 2}} \left\{ \left\| \begin{matrix} (I_n - qq^T)\bar{A}q \\ \bar{C}q \end{matrix} \right\| \right\}$$
 (A1.b)

The perturbation matrices $\Delta \bar{A}^*$ and $\Delta \bar{C}^*$ that make the original system unobservable are not directly available in terms of q * [14] but are needed for the applications proposed in this paper. Thus, they are derived in this appendix.

To be self-contained, algorithm 4 in [14] is summarized as the flow chart in Fig. A1. It uses algorithm 1, which is summarized as the flow chart in Fig. A2. Note that the minimum perturbation matrices are given in terms of intermediate variables Q and A_k and B_k as in Fig. A1. To stay consistent with the procedures used in [14], the derivation is first performed for controllability and then extended to observability using their duality. Note that the bars over the matrix notation are removed in this Appendix (i.e., $\Delta \bar{A}^* \rightarrow$

 ΔA^*) for simplicity. Only the derivation procedure for solving (A1.b) is given in this appendix because it can be easily extended to solve (A1.a).

6.1. Perturbation matrix, ΔA^* in terms of q^* and A

6.1.1 Problem formulation

Given (A2) from algorithm 4 in the controllability studies of [14], find the ΔA^* in terms of A and q^* that makes the system uncontrollable. Then, extend the result to observability studies to find $\Delta \bar{A}^*$ in terms of A and q^* .

$$\Delta A^* = Q A_{k0} Q^T - A \tag{A2}$$

where
$$A_k = Q^T A Q$$

$$= \begin{bmatrix} A_k (1:n-2, 1:n-2) & A_k (1:n-2, n-1:n) \\ A_k (n-1:n, 1:n-2) & A_k (n-1:n, n-1:n) \end{bmatrix}$$
(A3)

$$\begin{array}{c}
A_{k0} \\
\triangleq \begin{bmatrix} A_k(1:n-2,1:n-2) & A_k(1:n-2,n-1:n) \\
0 & A_k(n-1:n,n-1:n) \end{bmatrix}
\end{array} (A4)$$

$$\begin{aligned} 6.7.2 & \text{Solution} \\ (A4) &\Rightarrow A_{k0} = \begin{bmatrix} A_k(1:n-2,1:n-2) & A_k(1:n-2,n-1:n) \\ A_k(n-1:n,1:n-2) & A_k(n-1:n,n-1:n) \end{bmatrix} \\ &- \begin{bmatrix} 0 & 0 \\ A_k(n-1:n,1:n-2) & 0 \end{bmatrix} \\ &\stackrel{(A3)}{\Longrightarrow} A_{k0} = A_k - \begin{bmatrix} 0 & 0 \\ 0 & I_2 \end{bmatrix} A_k \begin{bmatrix} I_{n-2} & 0 \\ 0 & 0 \end{bmatrix} \stackrel{(A3)}{\Longrightarrow} (A5) \end{aligned}$$

$$A_{k0} = Q^T A Q - \begin{bmatrix} 0 & 0 \\ 0 & I_2 \end{bmatrix} Q^T A Q \begin{bmatrix} I_{n-2} & 0 \\ 0 & 0 \end{bmatrix}$$
 (A5)

$$\begin{aligned} (A2) &\Rightarrow \Delta A^* = QA_{k0}Q^T - A \\ &\stackrel{(A5)}{\Longrightarrow} \Delta A^* = -Q \begin{bmatrix} 0 & 0 \\ 0 & I_2 \end{bmatrix} Q^T A Q \begin{bmatrix} I_{n-2} & 0 \\ 0 & 0 \end{bmatrix} Q^T \\ &\Rightarrow \Delta A^* = -[0 \quad Q(:,n-1:n)] \begin{bmatrix} Q(:,1:n-2)^T \\ Q(:,n-1:n)^T \end{bmatrix} \\ A[Q(:,1:n-2) \quad 0] \begin{bmatrix} Q(:,1:n-2)^T \\ Q(:,n-1:n)^T \end{bmatrix} \\ &= -\{Q(:,n-1:n)Q(:,n-1:n)^T \} A \{Q(:,1:n-2)^T \} \\ &\underbrace{Q(:,1:n-2)Q(:,1:n-2)^T = I_n - Q(:,n-1:n)Q(:,n-1:n)^T}_{Q(:,1:n-2)Q(:,1:n-2)^T} \} \end{aligned}$$

$$\Delta A^* = -\{Q(:, n-1:n)Q(:, n-1:n)^T\}A$$

$$\{I_n - Q(:, n-1:n)Q(:, n-1:n)^T\}$$

$$= -\{q^*q^{*T}\}A\{I_n - q^*q^{*T}\}$$
(A6)

The observability duality of (A6) is (A7).

$$\Delta \bar{A}^* = -\{I_n - q^* q^{*T}\} A \{q^* q^{*T}\}$$
(A7)

6.2. Perturbation matrix ΔC^* in terms of q^* and C

6.2.1 Problem formulation

Given (A8), which is from the controllability studies, find ΔB^* in terms of B and q^* that makes the system uncontrollable. Then, extend the result to find ΔC^* in terms of C and q^* for observability analysis.

$$\Delta B^* = QB_{k0} - B \tag{A8}$$

where

$$B_k = Q^T B = \begin{bmatrix} B_k(1:n-2,:) \\ B_k(n-1:n,:) \end{bmatrix}$$
 (A9)

$$B_{k0} \triangleq \begin{bmatrix} B_{k_{(1:n-2,:)}} \\ 0 \end{bmatrix} \tag{A10}$$

6.2.2 Solution

$$(A10) \Rightarrow B_{k0} \triangleq \begin{bmatrix} B_{k(1:n-2,:)} \\ 0 \end{bmatrix} = \begin{bmatrix} I_{n-2} & 0 \\ 0 & 0 \end{bmatrix} \begin{bmatrix} B_{k(1:n-2,:)} \\ B_{k(n-1:n,:)} \end{bmatrix}$$
$$\stackrel{(A9)}{\Longrightarrow} B_{k0} = \begin{bmatrix} I_{n-2} & 0 \\ 0 & 0 \end{bmatrix} B_k \stackrel{(A9)}{\Longrightarrow} (A11)$$

$$B_{k0} = \begin{bmatrix} I_{n-2} & 0\\ 0 & 0 \end{bmatrix} Q^T B \tag{A11}$$

$$(A8) \rightarrow \Delta B^* = QB_{k0} - B$$

$$\stackrel{(A11)}{\Longrightarrow} \Delta B^* = Q \begin{bmatrix} I_{n-2} & 0 \\ 0 & 0 \end{bmatrix} Q^T B - B$$

$$= \left\{ Q \begin{bmatrix} I_{n-2} & 0 \\ 0 & 0 \end{bmatrix} Q^T - QQ^T \right\} B$$

$$= -Q \begin{bmatrix} 0 & 0 \\ 0 & I_2 \end{bmatrix} Q^T B \rightarrow (A12)$$

$$\Delta B^* = -Q(:, n-1:n)Q(:, n-1:n)^T B$$

= $-q^*q^{*T} B$ (A12)

The observability duality of (A12) is (A13).

$$\Delta C^* = -Cq^*q^{*T} \tag{A13}$$

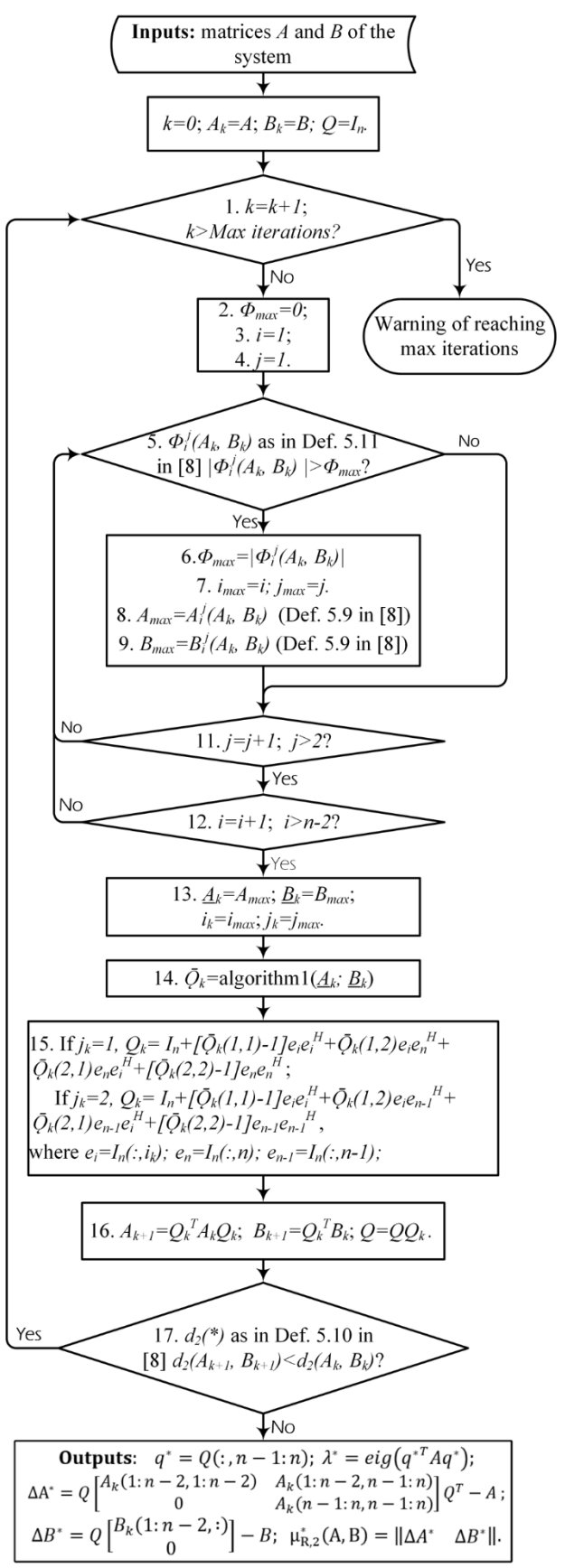


Fig. A1. Flow chart for calculating the minimum distance from a given system to an uncontrollable system through real number perturbation using algorithm 4 in [14]

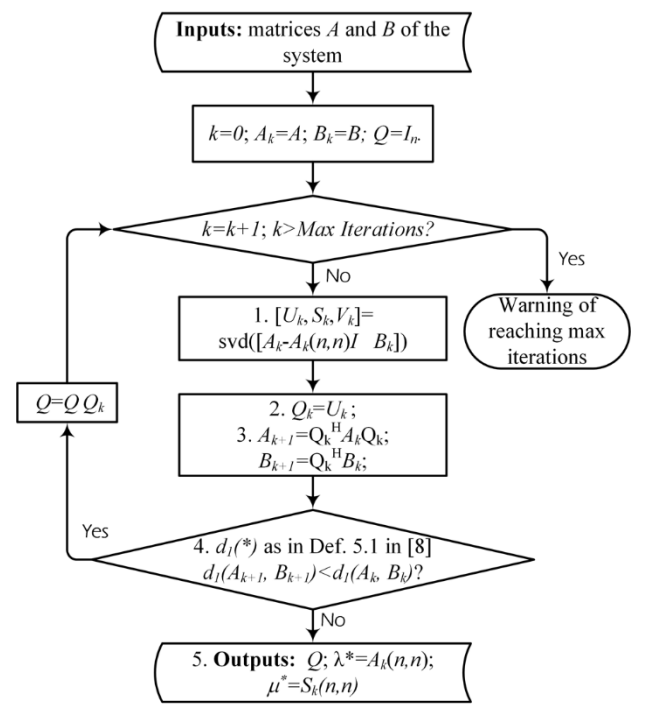


Fig. A2. Flow chart for calculating the minimum distance from a given system to an uncontrollable system through complex number perturbation using algorithm 1 in [14]

7. Acknowledgement

This paper is based on work sponsored by the U.S. Department of Energy (DOE) through its Advanced Grid Modeling program and U.S. National Science Foundation (NSF) through grant no. #1845523. Pacific Northwest National Laboratory is operated by Battelle for DOE under Contract DE-AC05-76RL01830.

8. References

- [1] J. Zhao, M. Netto, Z. Huang and e. al., "Roles of dynamic state estimation in power system modeling, monitoring and operation," *IEEE Transactions on Power Systems*, vol. 36, no. 3, pp. 2462-2472, 2020.
- [2] E. Ghahremani and I. Kamwa, "Local and wide-area PMU-based decentralized dynamic state estimation in multi-machine power systems," *IEEE Transactions on Power Systems*, vol. 31, no. 1, pp. 547-562, 2015.
- [3] S. Akhlaghi, N. Zhou and E. Wu, "PMU placement for state estimation considering measurement redundancy and controlled islanding," in *Proc. IEEE PES General Meeting*, Boston, MA, USA, 2016.
- [4] C.-T. Chen, "6.3 Observability," in *Linear System Theory and Design (3rd Edition)*, New York Oxford, Oxford University Press, September, 1998, pp. 153-158.
- [5] K. Sun, J. Qi and W. Kang, "Power system observability and dynamic state estimation for stability monitoring using synchrophasor measurements," *Control Eng. Prac.*, vol. 53, pp. 160-172, 2016.

- [6] A. Rouhani and A. Abur, "Measurement selection for observability in dynamic state estimation," in 2016 Power Systems Computation Conference (PSCC), Genoa, Italy, 2016.
- [7] A. Rouhani and A. Abur, "Observability analysis for dynamic state estimation of synchronous machines," *IEEE Trans. Power Syst.*, vol. 32, no. 4, pp. 3168-3175, 2017.
- [8] A. Abur, "Observability and dynamic state estimation," in 2015 IEEE Power & Energy Society General Meeting, Denver, Colorado, USA, 2015.
- [9] G. Wang, C. Liu, N. Bhatt, E. Farantatos and K. Sun, "Observability for PMU-based monitoring of nonlinear power system dynamics," in *Proc. 2013 IREP Symp. Bulk Power Syst. Dyn. Control—IX Optimization Security Control*, Rethymnon, Crete, Greece, Aug. 2013.
- [10] G. Wang, C. Liu, N. Bhatt, E. Farantatos and M. Patel, "Observability of nonlinear power system dynamics using synchrophasor data," *Int. Trans. Elect. Energy Syst.*, vol. 26, no. 5, pp. 952-967, May 2016.
- [11] J. Qi, K. Sun and W. Kang, "Optimal PMU placement for power system dynamic state estimation by using empirical observability Gramian," *IEEE Transactions* on *Power Systems*, vol. 30, no. 4, pp. 2041-2054, 2015.
- [12] N. Zhou, S. Wang, J. Zhao and Z. Huang, "Application of detectability analysis for power system dynamic state estimation," *IEEE Transactions on Power Systems*, vol. 35, no. 4, pp. 3274-3277, July 2020.
- [13] M. Maggiore, "Chapter 7. State estimation and output feedback control," in *Foundations of Linear Control Theory*, 2019, pp. 141-162.
- [14] M. Wicks and R. DeCarlo, "Computing the distance to an uncontrollable system," *IEEE Trans. Automat. Contr.*, vol. 36, no. 1, pp. 39-49, Jan 1991.
- [15] C. Paige, "Properties of numerical algorithms related to computing controllability," *IEEE Trans. Automat. Contr.*, vol. 26, no. 1, pp. 130-138, 1981.
- [16] E. Mengi, Measures for Robust Stability and Controllability, New York: PhD dissertation, New York University, Graduate School of Arts and Science, 2006.
- [17] M. Verhaegen and V. Verdult, "The asymptotic observer," in *Filtering and System Identification: a Least Squares Approach*, Cambridge University Press, 2007, pp. 128-133.
- [18] J. Kautsky, N. K. Nichols and P. V. Dooren, "Robust pole assignment in linear state feedback," *Int. J. Control*, vol. 41, no. 5, pp. 1129-1155, 1985.
- [19] P. Kundur, Power System Stability and Control, New York: McGraw-Hill, 1994.
- [20] J. Zhao and L. Mili, "Robust unscented Kalman filter for power system dynamic state estimation with unknown noise statistics," *IEEE Trans. Smart Grid*, vol. 10, no. 2, pp. 1215-1224, 2019.

- [21] L. Fan and Y. Wehbe, "Extended Kalman filtering based real-time dynamic state and parameter estimation using PMU data," *Electric Power Systems Research*, no. 103, pp. 168-177, 2013.
- [22] C. Canizares et al., IEEE Task Force on Benchmark Systems for Stability Controls, "Benchmark models for the analysis and control of small-signal oscillatory dynamics in power systems," *IEEE Transactions on Power Systems*, vol. 32, no. 1, pp. 715-722, 2017.
- [23] J. Zhao, S. Wang, N. Zhou, R. Huang, L. Mili and Z. Huang, "A new multi-scale state estimation framework for next generation of power grid EMS," in *Proc. IEEE PES General Meeting*, Atlanta, GA, USA, 2019.